



OPEN

Effect of weightbearing and foot positioning on 3D distal tibiofibular joint parameters

Firas Souleiman^{1,2,4}✉, Martin Heilemann^{1,2,3,4}, Robert Hennings^{1,2}, Pierre Hepp^{1,2}, Boyko Gueorguiev¹, Geoff Richards¹, Georg Osterhoff^{1,2} & Dominic Gehweiler¹

The aim of this study was to investigate the effect of different loading scenarios and foot positions on the configuration of the distal tibiofibular joint (DTFJ). Fourteen paired human cadaveric lower legs were mounted in a loading frame. Computed tomography scans were obtained in unloaded state (75 N) and single-leg loaded stand (700 N) of each specimen in five foot positions: neutral, 15° external rotation, 15° internal rotation, 20° dorsiflexion, and 20° plantarflexion. An automated three-dimensional measurement protocol was used to assess clear space (diastasis), translational angle (rotation), and vertical offset (fibular shortening) in each foot position and loading condition. Foot positioning had a significant effect on DTFJ configuration. Largest effects were related to clear space increase by 0.46 mm (SD 0.21 mm) in loaded dorsal flexion and translation angle of 2.36° (SD 1.03°) in loaded external rotation, both versus loaded neutral position. Loading had no effect on clear space and vertical offset in any position. Translation angle was significantly influenced under loading by -0.81° (SD 0.69°) in internal rotation only. Foot positioning noticeably influences the measurements when evaluating DTFJ configuration. Loading seems to have no relevant effect on native ankles in neutral position.

Syndesmotic injuries are associated with sprain or fractures of the ankle in up to 18% or 45% of the cases, respectively^{1–4}. For the general athletic population, rates of 10–20% have been reported⁵. Foot positioning is relevant for the pathomechanics of syndesmotic ankle injuries and appears to have a high impact on the distal tibiofibular joint (DTFJ) configuration, e.g. in dorsiflexion and external rotation injuries^{6–8}. Adequate reduction and stabilization are important to achieve a satisfying outcome with timely return to sport activities. To ensure anatomical reconstruction, identification of malpositioning is important. Numerous two-dimensional measurements for DTFJ assessment have been established^{9–13}. However, two-dimensional measurements represent a simplification of the geometry that is not justified considering the complexity of this joint^{14,15}. Therefore, three-dimensional (3D) measurement methods are becoming more popular as part of the technological development^{15–17}. Since the correct reduction of the fibula in the fibular notch of the tibia is the main factor for good functional long-term outcome and stability, accurate analysis of DTFJ is crucial^{18–22}.

Weightbearing cone-beam computed tomography (WBCT) is an alternative imaging technique allowing scanning under loading conditions with low radiation exposure²³. Initial studies using WBCT demonstrated promising results in terms of effectiveness in detecting syndesmosis injuries²⁴. Nevertheless, the benefit in the detection of syndesmotic lesions is discussed^{25–30}. Especially in the immediate post-traumatic and post-operative situation, the patients are unable to stand on the injured leg under full weightbearing because of pain. The systematic influence of foot position on DTFJ configuration in case of intact ligaments has not been sufficiently investigated^{31,32}. It is well known that bilateral imaging should be used for good DTFJ assessment due to interindividual differences^{9,15,33}. However, what is beneficial when using bilateral imaging if the position of both feet is different? Are there any systematic errors due to particular non-neutral foot positions? Therefore, the aim of this study was to investigate the effect and magnitude of different loading scenarios and foot positions on DTFJ configuration. It was hypothesized that both foot positioning and loading have a significant effect on this configuration despite intact ligaments.

¹AO Research Institute Davos, Davos, Switzerland. ²Department of Orthopaedics, Trauma and Plastic Surgery, University Hospital Leipzig, Leipzig, Germany. ³ZESBO—Center for Research On Musculoskeletal Systems, Leipzig University, Leipzig, Germany. ⁴These authors contributed equally: Firas Souleiman and Martin Heilemann. ✉email: frs.souleiman@medizin.uni-leipzig.de

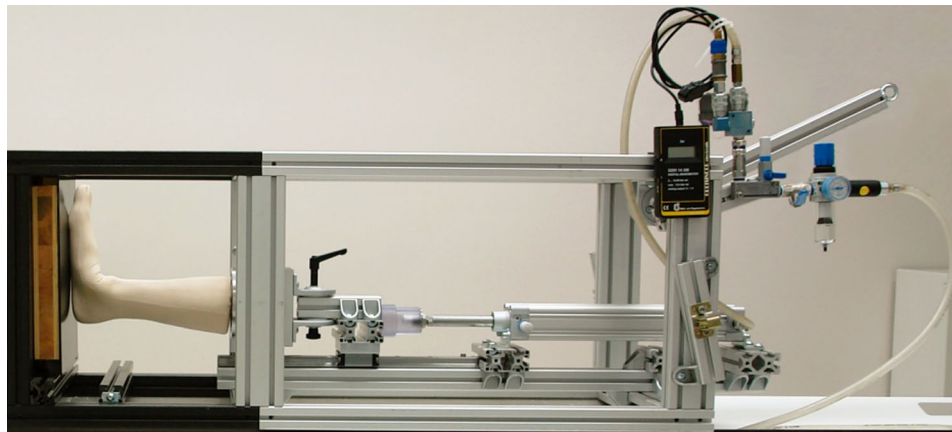


Figure 1. Custom-made loading frame with an artificial lower leg mounted for CT scanning under weightbearing in neutral foot position. The distal end of the frame is made out of radiolucent composite material, the main part is made out of aluminum. A pneumatic cylinder is connected to a compressed air system at the proximal end of the frame.



Figure 2. Wooden shanks used to maneuver the specimens in five foot positions in the loading frame during CT scanning; left to right: 15° external rotation, 15° internal rotation, neutral position, 20° plantar flexion, 20° dorsal flexion. The exemplified images are processed via volume rendering using Mimics Innovation Suite (Materialise, Leuven, Belgium).

Materials and methods

Fourteen paired fresh-frozen (-20°C) human cadaveric lower legs from four male and three female donors aged 81 years on average (range 59–91 years) with no visible preexisting pathology, trauma or surgery were used. After completion of the entire study, the integrity of ligamentous structures (syndesmotic ligaments) was surgically confirmed under visual control. The specimens were defrosted 24 h before preparation, then cut and embedded at the level of the middle tibia below the tuberosity in polymethylmethacrylate (PMMA; SCS-Beracryl, Suter-Kunststoffe AG, Fraubrunnen, Switzerland) with intact syndesmotic ligaments and membrana interossea. The fibula was cut at the level of embedding to be excluded from fixation. Each specimen was mounted horizontally in an air pressure-controlled radiolucent frame, specifically designed for positioning and axial loading of human cadaveric lower legs during computed tomography (CT) scanning (Fig. 1)³⁴.

The specimens were fixed in five different foot positions using wooden shanks—neutral (NP), 15° external rotation (ER), 15° internal rotation (IR), 20° dorsiflexion (DF), and 20° plantar flexion (PF) for CT scanning of each position in unloaded (75 N) and loaded (700 N) condition (Fig. 2). The two loading conditions are intended to simulate (1) unloaded single-leg stance—where only muscle forces are applied—and (2) fully loaded single-leg stance of an average person³⁴. The CT scans were performed with a slice thickness of 0.63 mm (SOMATOM Emotion 6, Siemens Healthcare GmbH, Erlangen, Germany). Following CT scanning, the Digital Imaging and Communications in Medicine (DICOM) data was processed in 3D Standard Triangle Language (STL) parts of the tibiae and fibulae using a standardized segmentation protocol (Mimics Innovation Suite, Materialise, Leuven, Belgium).

The STL data sets of the tibiofibular joints were evaluated using Matlab software package (MathWorks, Natick, MA, USA). For best possible comparability, the z-axis of the coordinate system was realigned for each foot in neutral position by determination of the tibia axis. The tibia axis was determined by calculation of the centroids of two tibial cross sections, located 50 mm and 80 mm proximally to the tibial articular surface, and represented by their connecting line.

In order to evaluate the effect of foot positioning on ankle joint parameters under the same axial loading condition (75 N or 700 N), each tibiofibular dataset in non-neutral positions (ER, IR, DF and PF) was matched to the data of the corresponding foot in neutral position using rigid iterative closest point algorithm based on

the respective tibial geometry. Consequently, alignment differences of the fibulae between the non-neutral and neutral foot positions became visible. These differences were quantitatively assessed by calculation of three 3D parameters defined in previous work: clear space difference (diastasis), vertical offset (fibular shortening), and translation angle (rotation)¹⁵. The translation angle was based on the combined anteroposterior and mediolateral displacement of the fibula around the tibia.

The clear space difference (ΔCS) between the corresponding tibiofibular joints was measured along the connecting line of the centroids of tibial and fibular cross sections located 10 mm proximal to the articular surface. The vertical offset (Δz) and translation angle ($\Delta \alpha$) were calculated from the connecting vector between tibial and fibular centers of volume. For calculation of the centers of volume, the tibia and fibula were virtually cut 20 mm proximal to the articular surface (distal tibial plafond), as the configuration of their distal ends is decisive for the anatomy of the tibiofibular joint. The translation angle mainly describes the anteroposterior translation of the fibula but can also be slightly influenced by mediolateral translation. Measurements of the vertical offset and translation angle on matched ankles is schematically visualized in Fig. 3.

To evaluate the effect of weightbearing in each separate position, the data of each loaded specimen (700 N) was best fit matched to its unloaded data (75 N) in the same position, followed by the same 3D measurements.

All parameters of interest were tested for normal distribution with Lilliefors test. Subsequently, clear space difference, vertical offset and translation angle were tested for significance using Paired-Samples t-test with post-hoc Holm-Bonferonni correction for multiple comparisons, since each parameter was tested for several foot positions and loading scenarios. Statistical analysis was performed at a level of significance 0.05 using Matlab.

Ethics approval. All experiments were carried out under the relevant guidelines and regulations. Additionally, the internal review boards at Science Care (Phoenix, AZ, USA) and AO Research Institute Davos (Davos, Switzerland) approved the study. This investigation was performed in accordance with the ethical standards as laid down in the Declaration of Helsinki (1964) and its later amendments or comparable ethical standards.

Consent to participate. All donors gave their informed consent inherent within the donation of the anatomical gift statement during their lifetime.

Consent for publication. All donors gave their informed consent inherent within the donation of the anatomical gift statement during their lifetime.

Results

Figure 4 visualizes clear space difference, vertical offset and translation angle for internal and external rotation, as well as for dorsal and plantar flexion, all relative to the corresponding neutral position. Mean value, standard deviation (SD) and p-value for each separate evaluated foot position and loading scenario are presented in Table 1.

Effect of foot position. The measurements demonstrated systematic errors due to particular foot positions compared to the neutral position for each of the three parameters of interest.

Clear space was significantly increased in IR (unloaded: $p = 0.001$, loaded: $p < 0.001$) and DF (unloaded: $p < 0.001$, loaded: $p < 0.001$). This parameter was most affected by DF under loading (mean difference: 0.46 mm, SD: 0.21 mm). ER and PF had no significant influences on the clear space ($p \geq 0.077$).

Significant proximal vertical offset was caused by IR (unloaded: $p = 0.019$, loaded: $p = 0.038$). Although the largest vertical offset was observed for PF under loading (mean: 0.41 mm, SD: 0.57 mm), this did not represent a significant change ($p = 0.449$). No significant influence on vertical offset was detected for ER and DF ($p \geq 0.177$).

Furthermore, ER caused significant translation of the fibula in dorsal direction (unloaded: $p < 0.001$, loaded: $p < 0.001$). Translation angle was most biased by ER under loading (mean: 2.36°, SD: 1.03°). No significant effect of foot position on translation angle was detected in IR, DF, and PF ($p \geq 0.341$).

Effect of loading. The comparisons of each separate foot position under loading versus the same position without loading resulted in no significant clear space difference ($p > 0.999$) and vertical offset ($p \geq 0.061$) among all specimens. Only in IR loading resulted in a significant translation angle (mean: -0.81° , SD: 0.69°, $p = 0.024$).

Discussion

In this study, CT imaging of human cadaveric lower legs revealed a significant effect of the foot position on clear space difference, vertical offset and translation angle, resulting in systematic errors of these DTFJ measures caused by non-neutral foot positioning during CT imaging. For this reason, the hypothesis that foot positioning considerably influences the DTFJ configuration with intact syndesmotic ligaments is confirmed. In contrast, the hypothesis that loading has an overall significant effect should be rejected.

In order estimate the extent of the systematic errors related to foot positioning, the outcomes of the current study need to be compared with thresholds for native anatomy. Native thresholds for clear space difference (± 2 mm), vertical offset (± 3 mm) and translation angle ($\pm 5^\circ$) were determined in previous work using the same 3D measurement method and are consistent with other findings in the literature^{9,15,35–37}. Comparing the parameter changes of the presented study to these thresholds, the translation angle was the most biased parameter influenced by foot positioning. A mean of 2.36° in dorsal direction for ER under loading corresponded to 47% of the threshold value. The difference for mean translation angle between ER and IR under loading was even 3.48°, accounting for 70% of the native threshold. Furthermore, the measured clear space increase of 0.46 mm

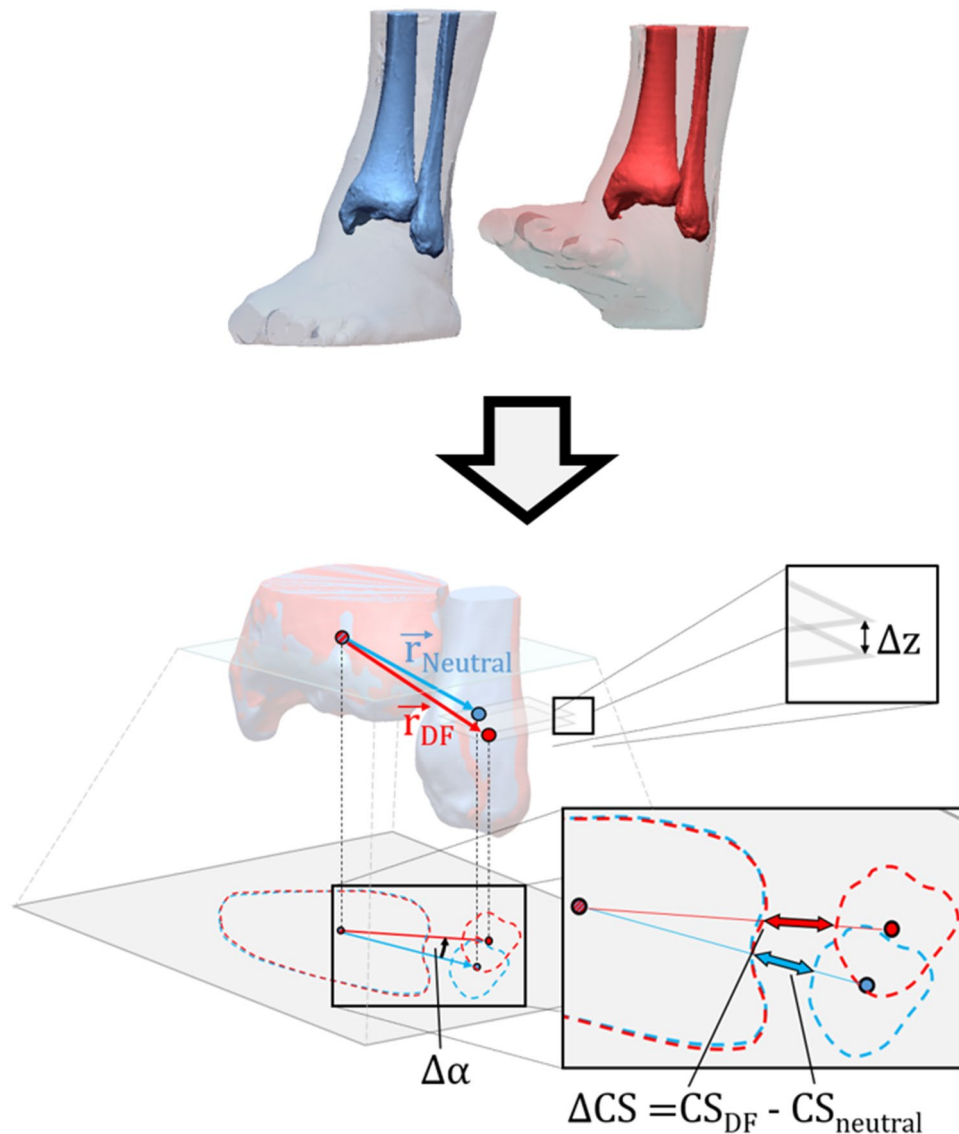


Figure 3. Matching (based on tibial geometry) and parameters calculation for an ankle in dorsal flexion relative to its neutral position. Clear space difference (ΔCS), vertical offset (Δz) and translation angle ($\Delta\alpha$) are determined by the connecting vectors ($\vec{r}_{Neutral}$, \vec{r}_{DF}) of the respective tibial and fibular centroids. The illustration was made using Geomagic Design X software (3D Systems, Rock Hill, SC, USA) and Microsoft PowerPoint (Microsoft, Redmond, WA, USA).

on average for DF under loading corresponded to 23% of the respective threshold value. Comparing the mean values for unloaded DF and PE, clear space differed by 0.82 mm equaling to 41% of the threshold. These large relative changes related to the thresholds for native anatomy demonstrated that rotation and flexion highly influence the fibula position along the frontal and sagittal axis. The current findings are consistent with a previous clinical study using mortise view radiographs to examine the medial clear space with respect to the foot position, where the authors reported significantly different syndesmosis widths between neutral position and different phases of plantar flexion³¹. An unloaded four-dimensional CT analysis could show similar effects of foot positioning³³. Changes in diastasis and fibular rotation were emphasized there, whereas the current work could additionally crystallize changes in sagittal translation.

The current study identified vertical offset explicitly in proximal direction. Only IR resulted in significant vertical offset change accounting for only 10% and 7% of the corresponding native threshold for this parameter in loaded and unloaded condition, respectively. Therefore, the vertical alignment of the fibula seems to be more stable against rotation and flexion than its alignment in the horizontal plane.

Furthermore, the 3D matching and evaluation of the lower legs in loaded and unloaded condition revealed almost no influence of loading on the clear space and vertical offset in the current study. Only in IR loading lead to a significant translation angle, however, the change accounted for only 16% of the native threshold, representing a much smaller effect than foot positioning. Such a minor influence of loading was also reported in a recent

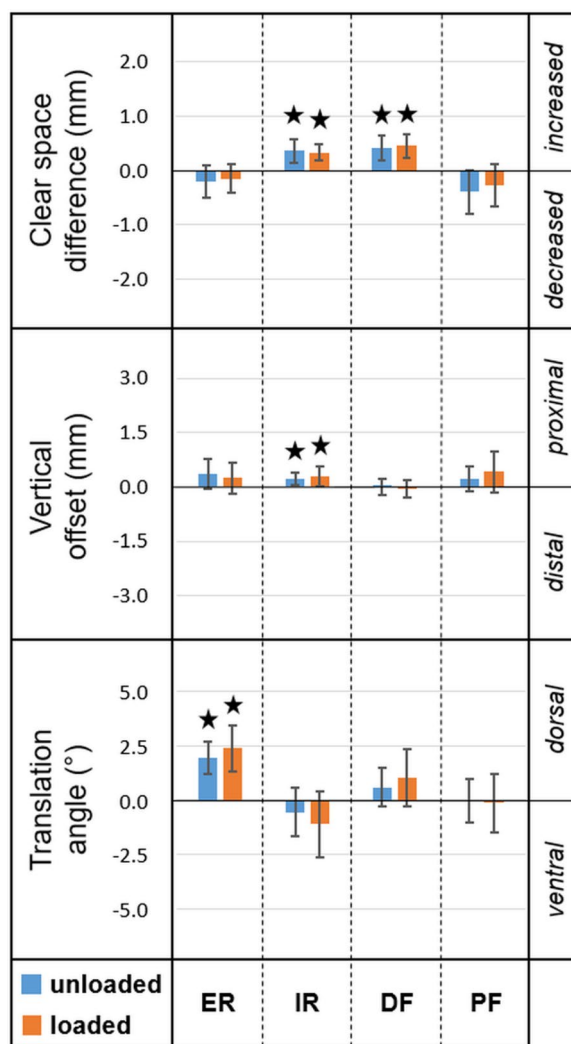


Figure 4. Clear space difference (ΔCS), vertical offset (Δz), and translation angle ($\Delta \alpha$) for each foot position relative to neutral position in either loaded or unloaded condition. Stars indicate significant differences. Axes are scaled to corresponding thresholds for native anatomy ($\Delta CS : \pm 2\text{mm}$, $\Delta z : \pm 3\text{mm}$, $\Delta \alpha : \pm 5^\circ$) in order to visualize relative extent of the respective measures¹⁵.

human cadaveric study designed with different severities of syndesmotic injury³⁰. In contrast, a meta analysis could demonstrate that imaging under loading can relevantly support detection of syndesmotic injury when the syndesmotic region is examined in detail³⁸. These contradictory findings confirm that further investigations focusing on well-selected parameters of interest are necessary. Three-dimensional positional control could provide crucial scientific benefits in this field too.

Overall, the current results revealed considerable influence of foot positioning on the tibiofibular parameters, whereas no relevant effect of loading on the clear space and vertical offset was observed, in particular for neutrally positioned ankles. Similarly, a human cadaveric study with injured syndesmotic ligaments also assessed the influence of axial loading and external rotation on the DTFJ configuration, reporting a considerable influence of external rotation compared to axial loading³⁹.

In recent years, the clinical use of WBCT for investigation of foot and ankle injuries has gained popularity⁴⁰. At a first glance, the advantages seem obvious with lower radiation exposure, faster feasibility (in case of available equipment), weightbearing and thus more physiological imaging^{40,41}. However, the benefit for assessment of the DTFJ configuration has to be questioned more critically due to the reported little influence of weightbearing. It remains questionable whether the small effect of weightbearing—even in injured state—results from the loading itself or is due to issues related to the used measurement methods³⁰. There is evidence that 3D position control is superior to previous two-dimensional measurements because the former better identifies the complexity of a joint malalignment^{14–17,42}. A good measurement response could already be proven for patients with disorders of the forefoot, midfoot, and hindfoot⁴⁰. Clinical studies using WBCT imaging in combination with 3D measurements to assess DTFJ configuration in injured state of the syndesmotic ligaments are currently pending. These might demonstrate a greater influence of weightbearing examinations than in the current study performed in

Matched specimen		Reference specimen		CS difference (mm)			Vertical offset (mm)			Translation angle (°)		
Position	Loading scenario	Position	Loading scenario	mean	SD	P-value	mean	SD	P-value	mean	SD	P-value
ER	Unloaded	Neutral	Unloaded	-0.20	0.30	0.540	0.35	0.41	0.177	1.96	0.75	<0.001
ER	Loaded	Neutral	Loaded	-0.15	0.26	0.968	0.24	0.43	0.968	2.36	1.03	<0.001
IR	Unloaded	Neutral	Unloaded	0.36	0.22	0.001	0.21	0.18	0.019	-0.58	1.12	>0.999
IR	Loaded	Neutral	Loaded	0.33	0.15	<0.001	0.29	0.26	0.038	-1.12	1.50	0.374
DF	Unloaded	Neutral	Unloaded	0.42	0.23	<0.001	0.01	0.23	>0.999	0.58	0.90	0.586
DF	Loaded	Neutral	Loaded	0.46	0.21	<0.001	-0.06	0.25	>0.999	1.01	1.32	0.341
PF	Unloaded	Neutral	Unloaded	-0.40	0.40	0.077	0.22	0.33	0.563	-0.03	0.43	>0.999
PF	Loaded	Neutral	Loaded	-0.26	0.39	0.562	0.41	0.57	0.449	-0.15	1.34	>0.999
Neutral	Loaded	Neutral	Unloaded	-0.06	0.18	>0.999	0.09	0.18	>0.999	-0.35	0.41	0.217
ER	Loaded	ER	Unloaded	0.03	0.12	>0.999	0.01	0.18	>0.999	0.12	0.49	>0.999
IR	Loaded	IR	Unloaded	-0.01	0.23	>0.999	0.22	0.21	0.051	-0.81	0.69	0.024
DF	Loaded	DF	Unloaded	-0.08	0.19	>0.999	0.09	0.18	>0.999	0.16	0.62	>0.999
PF	Loaded	PF	Unloaded	0.12	0.52	>0.999	0.29	0.44	0.583	-0.39	0.71	0.996

Table 1. Clear space (CS) difference, vertical offset, and translation angle in neutral position, external/internal rotation (ER/IR) and dorsal/plantar flexion (DF/PF), presented in terms of mean value and standard deviation (SD) for different loading scenarios together with the corresponding p-values from statistical comparisons.

intact specimen state⁴⁰. Corresponding 3D reference values for uninjured and injured state of the DTFJ exclusively in neutral foot position have to be determined. Such examinations were previously performed without consideration of the foot position¹⁵.

The results of this study demonstrate that foot positioning has a significantly greater influence on measured 3D parameters than loading in case of intact syndesmotom ligaments. This influence, including its quantitative dependence on foot positioning and loading, calculated by automatic 3D position control, has not been comprehensively elaborated to such an extent in any previous study. Changes of up to 70% of the native reference values in case of foot rotation are very high and could falsely influence the postoperative control. It has to be kept in mind that the internal and external rotation in the current study was limited to 15°. It is possible that a higher rotation could have resulted in even larger effects. In order to eliminate this error, the authors advocate the uniform use of a splint in neutral position. This is a cost-effective optimization of the measurement assessment and will lead to more comparable measurement values in the future. Especially in high performance athletes, who—as reported—are often affected by syndesmotom injuries, no mistakes should happen due to an incorrect measurement assessment. Numerous studies have described radiological malpositioning after surgical treatment of syndesmosis injuries^{18,20,43–45}. In retrospect, the imaging conditions under which the CT scans were performed must be analyzed.

To the best authors' knowledge, this is the first experimental study investigating in such detail the influence of rotation and flexion of the foot, as well as of weightbearing on the DTFJ configuration in case of intact syndesmotom ligaments. The current work has some limitations similar to those inherent to all cadaveric studies. A limited number of specimens was used. Static loads in constrained foot positions do not represent the complexity of human gait. It is possible that there are dynamic benefits of weightbearing recordings that could not be captured in the static examinations. Since this is a human cadaveric study, effects related to the lack of muscle activities cannot be excluded. Furthermore, for image acquisition in the CT frame it was necessary to perform a horizontal force application to the specimens. It can be assumed that some minor differences to the physiological stance are present. Furthermore, during preparation the tibia was resected at mid-shaft level, thus cutting off the proximal tibiofibular joint and excluding the fibula from the embedding. As a result, no direct force was applied to the fibula, which does not fully correspond to physiological conditions.

A major advantage of this work is the combination of CT scans in a loading frame, the use of a standardized segmentation protocol to create 3D bone models of the tibia and fibula, and an automated measurement procedure to calculate 3D parameters on the tibiofibular joint without rater-dependent detection of several landmarks. As the authors recommend the use of this beneficial measurement method in the future, the knowledge of the specific influence of foot position and loading, provided by this study, is essential.

In conclusion, a noticeable influence of foot positioning on the 3D DTFJ configuration was demonstrated using an automatic protocol. The loading seems to have no relevant effect on native lower legs in neutral position. Future studies could use the same 3D parameters to systematically investigate the effects of foot positioning and loading in case of syndesmotom ligament or other lesions of the foot and ankle.

Data availability

The datasets used and/or analyzed during the current study are available from the corresponding author on reasonable request.

Code availability

The code used during the current study are available from the corresponding author on reasonable request.

Received: 8 October 2021; Accepted: 6 May 2022

Published online: 07 June 2022

References

- Rammelt, S. & Obruba, P. An update on the evaluation and treatment of syndesmotic injuries. *Eur. J. Trauma Emerg. Surg.* **41**, 601–614 (2015).
- Steinmetz, S. *et al.* Tibiofemoral syndesmosis injury treated by temporary screw fixation and ligament repair. *Orthop. Traumatol. Surg. Res.* **102**, 1069–1073 (2016).
- Tornetta, P., Axelrad, T. W., Sibai, T. A. & Creevy, W. R. Treatment of the stress positive ligamentous SE4 ankle fracture: Incidence of syndesmotic injury and clinical decision making. *J. Orthop. Trauma* **26**, 659–661 (2012).
- Zalavras, C. & Thordarson, D. Ankle syndesmotic injury. *J. Am. Acad. Orthop. Surg.* **15**, 330–339 (2007).
- Gerber, J. P., Williams, G. N., Scoville, C. R., Arciero, R. A. & Taylor, D. C. Persistent disability associated with ankle sprains: A prospective examination of an athletic population. *Foot Ankle Int.* **19**, 653–660 (1998).
- Lauge-Hansen, N. Fractures of the ankle. V. Pronation-dorsiflexion fracture. *AMA Arch. Surg.* **67**, 813–820 (1953).
- Krähenbühl, N. *et al.* Impact of torque on assessment of syndesmotic injuries using weightbearing computed tomography scans. *Foot Ankle Int.* **40**, 710–719 (2019).
- Krähenbühl, N. *et al.* Torque application helps to diagnose incomplete syndesmotic injuries using weight-bearing computed tomography images. *Skelet. Radiol.* **48**, 1367–1376 (2019).
- Ahrberg, A. B. *et al.* Validation of a new method for evaluation of syndesmotic injuries of the ankle. *Int. Orthopaed. (SICOT)* **44**, 2095–2100 (2020).
- Carrara, C., Caravaggi, P., Belvedere, C. & Leardini, A. Radiographic angular measurements of the foot and ankle in weight-bearing: A literature review. *Foot Ankle Surg.* **26**, 509–517 (2020).
- Ebraheim, N. A., Lu, J., Yang, H., Mekhail, A. O. & Yeasting, R. A. Radiographic and CT evaluation of tibiofibular syndesmotic diastasis: A cadaver study. *Foot Ankle Int.* **18**, 693–698 (1997).
- Prior, C. P., Widnall, J. C., Rehman, A. K., Weller, D. M. & Wood, E. V. A simplified, validated protocol for measuring fibular reduction on ankle CT. *Foot Ankle Surg.* **23**, 53–56 (2017).
- Schon, J. M. *et al.* Defining the three most responsive and specific CT measurements of ankle syndesmotic malreduction. *Knee Surg. Sports Traumatol. Arthrosc.* **27**, 2863–2876 (2019).
- Kvarda, P. *et al.* High reliability for semiautomated 3D measurements based on weightbearing CT scans. *Foot Ankle Int.* **43**, 91–95 (2022).
- Souleiman, F. *et al.* A standardized approach for exact CT-based three-dimensional position analysis in the distal tibiofibular joint. *BMC Med. Imaging* **21**, 41 (2021).
- Burssens, A. *et al.* Templating of syndesmotic ankle lesions by use of 3D analysis in weightbearing and nonweightbearing CT. *Foot Ankle Int.* **39**, 1487–1496 (2018).
- Schon, J. M. *et al.* 3D model analysis of ankle flexion on anatomic reduction of a syndesmotic injury. *Foot Ankle Int.* **38**, 436–442 (2017).
- Naqvi, G. A., Cunningham, P., Lynch, B., Galvin, R. & Awan, N. Fixation of ankle syndesmotic injuries: Comparison of tigtrope fixation and syndesmotic screw fixation for accuracy of syndesmotic reduction. *Am. J. Sports Med.* **40**, 2828–2835 (2012).
- Nault, M.-L., Hébert-Davies, J., Laflamme, G.-Y. & Leduc, S. CT scan assessment of the syndesmosis: A new reproducible method. *J. Orthop. Trauma* **27**, 638–641 (2013).
- Sagi, H. C., Shah, A. R. & Sanders, R. W. The functional consequence of syndesmotic joint malreduction at a minimum 2-year follow-up. *J. Orthop. Trauma* **26**, 439–443 (2012).
- Vasarhelyi, A. *et al.* Detection of fibular torsional deformities after surgery for ankle fractures with a novel CT method. *Foot Ankle Int.* **27**, 1115–1121 (2006).
- Huyse, W. *et al.* Morphometric analysis of the incisura fibularis in patients with unstable high ankle sprains. *Skelet. Radiol.* **50**, 1141–1150 (2021).
- Richter, M., Seidl, B., Zech, S. & Hahn, S. PedCAT for 3D-imaging in standing position allows for more accurate bone position (angle) measurement than radiographs or CT. *Foot Ankle Surg.* **20**, 201–207 (2014).
- Bhimani, R. *et al.* Utility of volumetric measurement via weight-bearing computed tomography scan to diagnose syndesmotic instability. *Foot Ankle Int.* **41**, 859–865 (2020).
- Del Rio, A. *et al.* Weightbearing cone-beam computed tomography of acute ankle syndesmosis injuries. *J. Foot Ankle Surg.* **59**, 258–263 (2020).
- Hagemeijer, N. C. *et al.* Range of normal and abnormal syndesmotic measurements using weightbearing CT. *Foot Ankle Int.* **40**, 1430–1437 (2019).
- Hamard, M. *et al.* Accuracy of cone-beam computed tomography for syndesmosis injury diagnosis compared to conventional computed tomography. *Foot Ankle Surg.* **26**, 265–272 (2020).
- Osgood, G. M. *et al.* Reliability of distal tibio-fibular syndesmotic instability measurements using weightbearing and non-weight-bearing cone-beam CT. *Foot Ankle Surg.* **25**, 771–781 (2019).
- Shakoor, D. *et al.* Cone-beam CT measurements of distal tibio-fibular syndesmosis in asymptomatic uninjured ankles: Does weight-bearing matter?. *Skelet. Radiol.* **48**, 583–594 (2019).
- Krähenbühl, N. *et al.* Is load application necessary when using computed tomography scans to diagnose syndesmotic injuries? A cadaver study. *Foot Ankle Surg.* **26**, 198–204 (2020).
- Baumfeld, D. *et al.* Does Foot Position and Location of Measurement Influence Ankle Medial Clear Space?. *Foot Ankle Spec.* **11**, 32–36 (2018).
- Park, S. S., Kubiak, E. N., Egol, K. A., Kummer, F. & Koval, K. J. Stress radiographs after ankle fracture: the effect of ankle position and deltoid ligament status on medial clear space measurements. *J. Orthop. Trauma* **20**, 11–18 (2006).
- Wong, M. T., Wiens, C., Lamothe, J., Edwards, W. B. & Schneider, P. S. Four-Dimensional CT Analysis of Normal Syndesmotic Motion. *Foot Ankle Int.* **42**, 1491–1501 (2021).
- Hagen, J. E. *et al.* Comparison of ligament-repair techniques for the syndesmosis: A simulated cadaveric weight-bearing computed tomography analysis. *J. Foot Ankle Surg.* **59**, 1156–1161 (2020).
- Berkes, M. B. *et al.* Articular congruity is associated with short-term clinical outcomes of operatively treated SER IV ankle fractures. *J. Bone Jt. Surg. Am.* **95**, 1769–1775 (2013).
- Davidovitch, R. I. *et al.* Intraoperative syndesmotic reduction: Three-dimensional versus standard fluoroscopic imaging. *J. Bone Jt. Surg.* **95**, 1838–1843 (2013).
- Thordarson, D. B., Motamed, S., Hedman, T., Ebramzadeh, E. & Bakshian, S. The effect of fibular malreduction on contact pressures in an ankle fracture malunion model. *J. Bone Jt. Surg. Am.* **79**, 1809–1815 (1997).
- Raheman, F. J. *et al.* Can weightbearing cone-beam CT reliably differentiate between stable and unstable syndesmotic ankle injuries? A systematic review and meta-analysis. *Clin. Orthop. Relat. Res.* <https://doi.org/10.1097/CORR.0000000000002171> (2022).
- Burssens, A. *et al.* Comparison of external torque to axial loading in detecting 3-dimensional displacement of syndesmotic ankle injuries. *Foot Ankle Int.* **41**, 1256–1268 (2020).

40. Barg, A. *et al.* Weightbearing computed tomography of the foot and ankle: Emerging technology topical review. *Foot Ankle Int.* **39**, 376–386 (2018).
41. Mettler, F. A., Huda, W., Yoshizumi, T. T. & Mahesh, M. Effective doses in radiology and diagnostic nuclear medicine: A catalog. *Radiology* **248**, 254–263 (2008).
42. Burssens, A. *et al.* Interaction of loading and ligament injuries in subtalar joint instability quantified by 3D weightbearing computed tomography. *J. Orthop. Res.* **40**, 933–944 (2022).
43. Dikos, G. D., Heisler, J., Choplin, R. H. & Weber, T. G. Normal tibiofibular relationships at the syndesmosis on axial CT imaging. *J. Orthop. Trauma* **26**, 433–438 (2012).
44. Gardner, M. J., Demetrakopoulos, D., Briggs, S. M., Helfet, D. L. & Lorich, D. G. Malreduction of the tibiofibular syndesmosis in ankle fractures. *Foot Ankle Int.* **27**, 788–792 (2006).
45. Warner, S. J. *et al.* The measurement and clinical importance of syndesmotic reduction after operative fixation of rotational ankle fractures. *J. Bone Jt. Surg. Am.* **97**, 1935–1944 (2015).

Author contributions

F.S.: Concept and design of the investigation; data acquisition, analysis and interpretation; manuscript drafting. M.H.: Concept and design of the investigation; application of the developed measurement methodology to the data sets; writing automated scripts; manuscript drafting. R.H.: data acquisition, analysis and interpretation; manuscript drafting. P.H., G.R.: data analysis and interpretation; manuscript reviewing. B.G., G.O.: data analysis and interpretation; manuscript drafting and reviewing. D.G.: Concept and design of the work; data analysis and interpretation; manuscript reviewing. All authors read and approved the final manuscript.

Funding

Open Access funding enabled and organized by Projekt DEAL. The authors received no financial support for the research, authorship, and/or publication of this article.

Competing interests

The authors declare no competing interests.

Additional information

Correspondence and requests for materials should be addressed to F.S.

Reprints and permissions information is available at www.nature.com/reprints.

Publisher's note Springer Nature remains neutral with regard to jurisdictional claims in published maps and institutional affiliations.



Open Access This article is licensed under a Creative Commons Attribution 4.0 International License, which permits use, sharing, adaptation, distribution and reproduction in any medium or format, as long as you give appropriate credit to the original author(s) and the source, provide a link to the Creative Commons licence, and indicate if changes were made. The images or other third party material in this article are included in the article's Creative Commons licence, unless indicated otherwise in a credit line to the material. If material is not included in the article's Creative Commons licence and your intended use is not permitted by statutory regulation or exceeds the permitted use, you will need to obtain permission directly from the copyright holder. To view a copy of this licence, visit <http://creativecommons.org/licenses/by/4.0/>.

© The Author(s) 2022